Logarithmic coarsening in the Coulomb glass

Preeti Bhandari,[1,2] Vikas Malik,[3] and Sanjay Puri[1]
[1]*School of Physical Sciences, Jawaharlal Nehru University, New Delhi 110067, India*
[2]*Department of Physical Sciences, Indian Institute of Science Education and Research, Mohali 140306, India*
[3]*Department of Physics and Material Science, Jaypee Institute of Information Technology, Uttar Pradesh 201309, India*

(Received 16 January 2019; published 13 May 2019)

We present numerical results from a comprehensive Monte Carlo study in two dimensions ($d = 2$) of coarsening kinetics in the Coulomb glass (CG) model at half-filling. The CG model is characterized by spin-spin interactions which are long-range Coulombic and antiferromagnetic. For the nonequilibrium properties studied by us (spatial correlation functions and domain growth laws), we find that domain growth in the CG is analogous to that in the nearest-neighbor random-field Ising model. The domain length scale $L(t)$ shows a crossover from a regime of "power-law growth with a disorder-dependent exponent" [$L(t) \sim t^{1/\bar{z}}$] to a regime of "logarithmic growth with a universal exponent" [$L(t) \sim (\ln t)^{1/\psi}$].

DOI: 10.1103/PhysRevE.99.052113

I. INTRODUCTION

Consider the far-from-equilibrium evolution of a disordered system, which is rendered thermodynamically unstable by a rapid quench below the critical temperature (T_c). Clearly, the system does not order instantaneously; rather small domains of different symmetry grow with time to reach the new equilibrium state. This evolution is usually referred to as "phase ordering dynamics" or "domain growth" or "coarsening" [1,2]. The evolution towards equilibrium depends critically on whether or not the order parameter is conserved [1]. Phase ordering in a pure system is well documented in the literature [1–3].

Experimentally, the study of coarsening in systems becomes more relevant by introducing quenched disorder which is always present in real systems. In the presence of disorder, one would expect a slower dynamics due to trapping of domain walls by the disorder sites. Using scaling arguments, Lai *et al.* (LMV) [4] and others [5,6] have predicted a crossover from power-law growth at early times to logarithmic growth at late times. This scenario has proven very difficult to confirm, especially in the context of logarithmic growth [7,8]. Recently, some very interesting results on domain growth in the random-bond Ising model (RBIM) and random-field Ising model (RFIM) have been presented by Corberi *et al.* [9,10]. They have developed novel scaling arguments and numerical methods to demonstrate a crossover from power law to logarithmic growth in the RFIM and RBIM. In the power law regime, the exponent depends upon the disorder amplitude [8–10].

These studies have been restricted to systems with short-ranged (nearest-neighbor or NN) interactions. In this paper, we turn our attention to coarsening in an experimentally important system with long-ranged interactions and quenched disorder, i.e., the Coulomb glass (CG) at half-filling. The CG [11] is the standard model for disordered insulators, where the electronic states are localized at low temperatures due to the presence of disorder. These localized states are unable to screen the Coulomb interactions effectively. Most of the theoretical and experimental work [12,13] on the CG has focused on the high-disorder regime, where disorder and interactions are comparable. It is still controversial whether there is a glassy phase at high disorder and low temperature. Nonequilibrium studies of this model at high disorder show glassy properties such as slow relaxation [14–16], aging [17–20], and memory effects [21,22]. In this regime, a soft gap in the density of states is observed at low temperatures, which is termed the *Coulomb gap* [11]. This gives rise to the Efros-Shklovskii $T^{1/2}$ law for conductivity at low temperatures. As the temperature is increased, the gap gets filled up and the conductivity obeys the Mott $T^{1/4}$ law [12,13].

From the perspective of statistical physics, the CG is an antiferromagnetic (AF) Ising model with "spins" interacting via long-ranged Coulombic interactions. Disorder is introduced via random on-site energies. At zero disorder (for $d = 2, 3$) [23], the system undergoes a second-order phase transition from a paramagnetic to AF state as the temperature is lowered. It was also shown [23] that the critical exponents of the CG and the NN Ising model with AF ordering are the same in $d = 2, 3$. At finite disorder, Goethe *et al.* [24] showed that the $d = 3$ CG model has a similar phase diagram as the $d = 3$ NN-RFIM. At disorder $W < W_c$ (critical disorder), the $d = 3$ CG has AF ordering for $T < T_c(W)$. For the $d = 2$ CG model, two of us have argued [25] that a similar phase diagram may exist. In particular, Bhandari *et al.* [26] have shown that, for $0 \leqslant W < W_c$, there is AF ordering at $T = 0$ for the $d = 2$ CG. (This should be contrasted with the $d = 2$ NN-RFIM, where $W_c = 0$ [27,28]).

It is experimentally relevant to examine whether the nonequilibrium properties of the CG are also analogous to the corresponding NN models. In this context, we undertook this study of coarsening in the CG. Our paper is organized as follows. In Sec. II, the CG model is introduced and we present details of the numerical techniques used here. In Sec. III, we discuss domain growth laws and the scaling framework used for understanding phase ordering systems. In Sec. IV,

 ©2019 American Physical Society

we present our numerical results for the $d = 2$ CG. Finally, in Sec. V, we conclude this paper with a summary and discussion of our results.

II. COULOMB GLASS MODEL AND NUMERICAL DETAILS

Efros and Shklovskii [11] introduced the CG model for disordered insulators, where the electronic states are localized around the sites of a lattice of size $N = L^d$. Here, d is the dimensionality and L is the lateral size. The Hamiltonian for such a model in dimensionless units is defined as

$$\mathcal{H}\{n_i\} = \frac{1}{2}\sum_{i\neq j}\frac{e^2}{\kappa|\vec{r}_i - \vec{r}_j|}(n_i - 1/2)(n_j - 1/2) + \sum_{i=1}^{N} h_i n_i. \tag{1}$$

Here, $n_i \in \{0, 1\}$ is the electron occupation number and h_i is the random energy on site i. The interaction term corresponds to repulsive Coulombic interactions between electrons localized at sites i and j in a medium of dielectric constant κ.

We map the Hamiltonian in Eq. (1) into spin language by defining a pseudospin variable $S_i = n_i - 1/2$:

$$\mathcal{H}\{S_i\} = \frac{1}{2}\sum_{i\neq j} J_{ij}S_iS_j + \sum_{i=1}^{N} h_iS_i, \quad S_i = \pm 1/2. \tag{2}$$

This is identified as an Ising model with long-ranged AF interactions ($J_{ij} = e^2/\kappa r_{ij}$) and an on-site random field energy h_i. The field variables are taken from a uniform distribution $P(h)$, given by

$$\begin{aligned} P(h) &= 1/W, \quad -W/2 \leqslant h \leqslant W/2, \\ &= 0, \quad \text{otherwise}, \end{aligned} \tag{3}$$

where W is the strength of disorder. We focus on the case of half-filling, i.e., the number of electrons ($S_i = 1/2$) is equal to the number of holes ($S_i = -1/2$). Such a system possesses an electron-hole symmetry which gives chemical potential $\mu = 0$. Since the number of electrons is conserved, the total magnetization of the system is also conserved. However, the magnetization is not a suitable order parameter for this problem. In the absence of disorder ($W = 0$), the minimum-energy configuration or ground state of the Hamiltonian in Eq. (2) at half-filling is a checkerboard state (AF order), i.e., ..., electron, hole, electron, hole, ...

A schematic phase diagram of the $d = 2$ CG is shown in Fig. 1—this is based on the discussion in Refs. [25,26]. At zero and small values of W, the ground state of this system has AF ordering for $T < T_c(W)$. Therefore, the appropriate order parameter is the staggered magnetization, which is the difference between two sublattice magnetizations. This is defined as

$$\sigma = \frac{1}{N}\sum_{i=1}^{N}\sigma_i. \tag{4}$$

Here, the staggered spins σ_i are related to S_i as

$$\sigma_i = (-1)^{i_x+i_y}S_i, \tag{5}$$

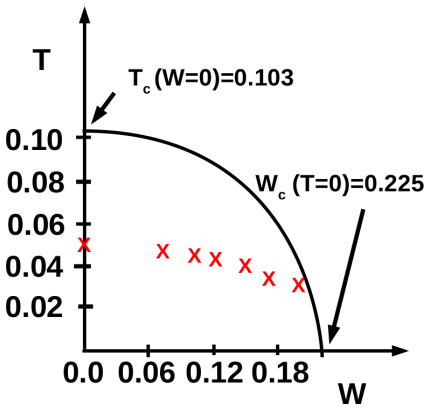

FIG. 1. Schematic phase diagram of the $d = 2$ Coulomb glass (CG) in the (W, T) plane. Our Monte Carlo (MC) simulations are performed at the points marked X.

where i_x, i_y denote the x, y coordinates of the site i. Energies and temperatures of the system are calculated in units of $e^2/\kappa a$, where a is the lattice constant.

In this paper, we have performed Monte Carlo (MC) simulations on a square lattice ($d = 2$) to study domain growth in the CG. Since the system has AF ordering, a domain consists of a cluster of spins with the same σ_i. From the phase diagram in Fig. 1, the two critical points along the zero-disorder line [23] and zero-temperature line [26] are already known. We have done our analysis for $0 \leqslant W < W_c(T = 0)$.

The details of the simulation are as follows. We choose the system size to be 512^2, and employ periodic boundary conditions in both directions. To cope with the long-range Coulomb interactions, we have used the Ewald summation technique [29].We assign random initial orientations to each site, i.e., $N/2$ randomly chosen sites have $S_i = 1/2$, and the remaining $N/2$ sites have $S_i = -1/2$. The system is rapidly quenched at time $t = 0$ from the high-temperature [$T > T_c(W)$] disordered state to a low temperature [$T < T_c(W)$], where the equilibrium system is ordered. The (W, T) values for our simulations are marked in Fig. 1. Since the total magnetization of the system is conserved, we study the phase ordering process via Kawasaki spin-exchange kinetics [1]. Thus the total magnetization (which is zero for the half-filling case) remains conserved, but the order parameter (staggered magnetization) is not conserved.

The MC technique with spin exchange and a Metropolis algorithm [30,31] proceeds as follows. A pair of opposite spins S_i and S_j (which are nearest neighbors) is chosen at random for spin exchange. This exchange is accepted with probability p, given by

$$\begin{aligned} p &= 1, \quad \Delta\mathcal{H} \leqslant 0, \\ &= e^{-\beta\Delta\mathcal{H}}, \quad \Delta\mathcal{H} > 0. \end{aligned} \tag{6}$$

Here,

$$\begin{aligned} \Delta\mathcal{H} = (S_i - S_j)\left(\sum_{k\neq i,j} J_{jk}S_k + h_j\right) \\ + (S_j - S_i)\left(\sum_{k\neq i,j} J_{ik}S_k + h_i\right) \end{aligned} \tag{7}$$

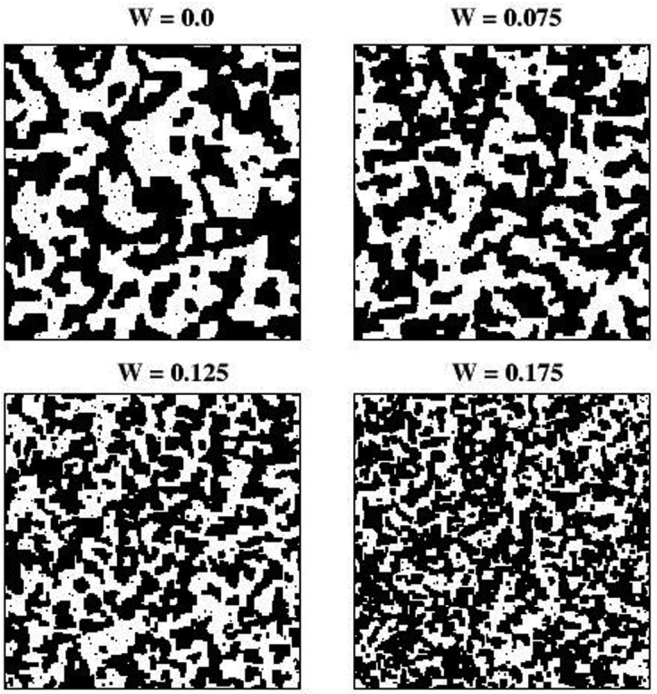

FIG. 2. Domain growth in the $d = 2$ CG at different disorder strengths. We show snapshots at $t = 10^3$ MCS for a lattice size of 512^2. The order parameter is the staggered magnetization $\sigma_i = (-1)^{i_x+i_y} S_i$. The black and white regions correspond to $\sigma_i > 0$ and $\sigma_i < 0$, respectively.

is the change in energy due to the spin exchange and $\beta = (k_B T)^{-1}$ (Boltzmann constant $k_B = 1$).

A single Monte Carlo step (MCS) corresponds to N attempted updates. All statistical data presented in this paper has been averaged over 50 independent runs. Each run had an independent initial condition $\{S_i\}(t = 0)$ and disorder configuration $\{h_i\}$. Since $W_c(T = 0) \simeq 0.225$ [26], the highest disorder amplitude chosen was $W = 0.20$. In Fig. 2, we show evolution snapshots of the staggered magnetization at a fixed time ($t = 10^3$ MCS) for different disorder amplitudes. We see that the domain growth is slower for larger values of disorder, due to the trapping of domains by disorder sites.

The important physical process of phase separation or spinodal decomposition is modeled by the ferromagnetic Ising model with Kawasaki kinetics [1]. In this case, the system is characterized by a conserved order parameter, and the domains are rich in up spins or down spins. The formation of large domains leads to frequent picking up of neighboring spins of the same sign in an MC simulation. Sophisticated algorithms [32] have been designed to overcome this problem. In our study, a domain has NN spins of opposite signs due to AF ordering and the above problem does not arise.

III. SCALING FUNCTIONS AND DOMAIN GROWTH LAWS

Domain growth is often characterized by the equal-time correlation function [1]:

$$C(\vec{r}, t) = \frac{1}{N} \sum_{i=1}^{N} [\langle \sigma_i(t)\sigma_j(t)\rangle - \langle \sigma_i(t)\rangle\langle \sigma_j(t)\rangle]. \quad (8)$$

Here, $\vec{r} = \vec{r}_i - \vec{r}_j$ is the fixed distance between the staggered spins σ_i and σ_j. The angular brackets in Eq. (8) denote an average over independent runs.

The growth process is characterized by a unique length scale $L(t)$, which grows with time and becomes the dominant length scale (see Fig. 2). One can then rescale all other lengths with respect to $L(t)$. In that case, the correlation function for an isotropic system has the scaling form [1]

$$C(r, t) = f\left(\frac{r}{L(t)}\right). \quad (9)$$

Equation (9) reflects the fact that the morphology of the domains is invariant in time, but the scale of the morphology grows as $L(t)$. We define $L(t)$ as the distance over which $C(r, t)$ decays to some fraction of its maximum value. The NN AF Ising model at half-filling with Kawasaki kinetics (conserved magnetization but nonconserved order parameter σ) is equivalent to the NN ferromagnetic Ising model with Glauber (nonconserved) kinetics [33]. In that case, the scaling function $f(x)$ is well described by the Ohta-Jasnow-Kawasaki (OJK) function [34]:

$$f_{\rm OJK}(x) = \frac{2}{\pi} \sin^{-1}\left(e^{-x^2}\right). \quad (10)$$

Next we discuss the time dependence of the domain growth law. In the case of a pure and isotropic system having short-range interactions, growth laws are well understood [1–3]. In the NN Ising model with nonconserved kinetics, the system follows the Lifshitz-Cahn-Allen (LCA) law, $L(t) \sim t^{1/2}$. For the same model with conserved kinetics, it follows the Lifshitz-Slyozov (LS) growth law, $L(t) \sim t^{1/3}$.

As we have mentioned earlier, the scenario is different when disorder is included. In this case, the domain walls are trapped by disorder sites, which results in the slow growth of $L(t)$, which often shows logarithmic time dependence. An interesting work in this context is due to Corberi *et al.* [10], who studied nonconserved coarsening in the $d = 2, 3$ RFIM. They developed a novel framework to characterize the crossover from power law to logarithmic growth. The primary aim of this paper is to study the late stages of domain growth in the CG, using the framework developed by Corberi *et al.*

Lai *et al.* (LMV) [4] have undertaken a systematic study of phase ordering in the case of nonconserved kinetics. In the LMV scheme, the domain growth law in models with NN interactions obeys

$$\frac{dL}{dt} = \frac{D(L, T)}{L}. \quad (11)$$

Here, $D(L, T)$ is the diffusion constant which, in general, depends upon the domain scale and temperature (T). For the pure Ising case, $D(L, t) = D_0$ (constant), which gives the LCA growth law: $L(t) = (2D_0 t)^{1/2}$. For the disordered system, domain growth proceeds via thermal activation over energy barriers (E_B), so

$$D(L, T) \simeq D_0 \exp(-E_B/T). \quad (12)$$

At late times, due to the pinning of domains at certain locations, the energy barriers of the disordered system scale as

$$E_B(L) \sim W L^{\psi}, \quad (13)$$

where W is the disorder amplitude and ψ is an exponent which depends on the pinning and roughness of domains [5,6,35]. Therefore, the typical diffusion constant for barrier hopping is

$$D(L,T) \simeq D_0 \exp\left(-\frac{W}{T}L^{\psi}\right). \tag{14}$$

Replacing this is Eq. (11), we find that domain growth is described by a crossover behavior [6]

$$L(t) \simeq L_0(T,W)h\left(\frac{t}{t_0}\right), \tag{15}$$

where

$$\begin{aligned} L_0(T,W) &= \left(\frac{T}{W}\right)^{1/\psi}, \\ t_0(T,W) &= \frac{1}{D_0\psi}\left(\frac{T}{W}\right)^{2/\psi}. \end{aligned} \tag{16}$$

Notice that $L_0, t_0 \to \infty$ when $W \to 0$, as expected. The crossover function is

$$\begin{aligned} h(x) &= \left(\frac{2}{\psi}x\right)^{1/2}, \quad x \ll 1, \\ &= (\ln x)^{1/\psi}, \quad x \gg 1. \end{aligned} \tag{17}$$

In related work, Shore *et al.* [36] showed that a system can have L-dependent barriers even in the absence of disorder. They considered an Ising ferromagnet with weak next-nearest-neighbor (NNN) AF bonds. These AF bonds create energy barriers which greatly slow down domain growth. Their $d = 2$ and $d = 3$ models correspond to $\psi = 0$ and $\psi = 1$, respectively.

The asymptotic logarithmic behavior has proven elusive in numerical simulations [7]. An extensive MC study of the nonconserved RBIM was undertaken by Paul *et al.* [8]. These authors reported a power-law growth with an exponent which depends on the disorder amplitude. Their results were consistent with energy barriers which grow logarithmically with the length scale, rather than the power-law barriers discussed above. Paul *et al.* argued that the energy barriers of the disordered system scale as

$$E_B(L) \sim W \ln(1+L). \tag{18}$$

Replacing this in Eq. (12), the diffusion constant is

$$D(L,T) \simeq D_0(1+L)^{-W/T}. \tag{19}$$

Then, using Eq. (11), the corresponding growth law is

$$L(t) \sim t^{1/\bar{z}}, \tag{20}$$

where $\bar{z} = 2 + W/T$.

In recent work, Corberi *et al.* [9,10] have demonstrated that the above regime is an intermediate growth regime, which is followed by an asymptotic logarithmic regime. They have developed an innovative method of analyzing the growth data, which we briefly summarize here. They propose the following scaling form for the growth law:

$$L(t,W) \sim t^{1/z_{\rm eff}} = t^{1/z}F\left(\frac{W}{T}t^{\phi}\right). \tag{21}$$

Here, $z_{\rm eff}$ is the effective growth exponent, $z = 2$ is the pure growth exponent, and $\phi > 0$ is the crossover exponent. The crossover time scales as $t_0 \sim (W/T)^{-1/\phi}$. The scaling function $F(x = Wt^{\phi}/T)$ behaves as

$$\begin{aligned} F(x) &= \text{const}, \quad x \to 0, \\ &= x^{-1/(\phi z)}\mathcal{L}(x^{1/\phi}), \quad x \to \infty, \end{aligned} \tag{22}$$

where $\mathcal{L}(x)$ is a universal function of its argument.

To evaluate the effective growth exponent, it is more convenient to use the inverted form of Eq. (21):

$$t = L^z G(L/\lambda), \tag{23}$$

where the crossover length scale $\lambda = (W/T)^{-1/(\phi z)} = t_0^{1/z}$. The scaling functions $G(y = L/\lambda)$ and $F(x = Wt^{\phi}/T)$ are related as

$$G(y) = [F(x)]^{-z}. \tag{24}$$

The corresponding scaling form of the diffusion constant is obtained from Eq. (11) as

$$\begin{aligned} D(L,T) &= L\frac{dL}{dt} \\ &= [zL^{z-2}G(L/\lambda) + L^{z-1}G'(L/\lambda)/\lambda]^{-1}. \end{aligned} \tag{25}$$

The effective growth exponent as a function of y is obtained from Eq. (23) as

$$z_{\rm eff}(y) = \frac{\partial(\ln t)}{\partial(\ln L)} = z + \frac{\partial(\ln G)}{\partial(\ln y)}. \tag{26}$$

Thus we expect $z_{\rm eff} - z$ to be a universal function of y. We generalize Eqs. (21)–(26) by replacing z (pure case) with $\bar{z}$, which is dependent on W and T. Corberi *et al.* [9,10] argue that a power-law dependence of this function implies an exponential dependence of $G(y)$:

$$\frac{\partial(\ln G)}{\partial(\ln y)} = by^{\psi} \to G(y) \sim \exp\left(\frac{b}{\psi}y^{\psi}\right). \tag{27}$$

Notice that we have deliberately used the same symbol (ψ) for the barrier-scaling exponent in Eq. (13) and the power-law exponent in Eq. (27). Replacing $G(y)$ from Eq. (27) in Eq. (23) yields an asymptotic logarithmic growth:

$$\frac{L}{\lambda} = \left[\frac{\psi}{b}\ln\left(\frac{t}{\lambda^{\bar{z}}}\right)\right]^{1/\psi}. \tag{28}$$

IV. NUMERICAL RESULTS

In Fig. 2, we show evolution morphologies of the CG model at $t = 10^3$ MCS for $W = 0.0, 0.075, 0.125, 0.175$. The pictures show the staggered magnetization, which is the appropriate order parameter in this context. From these snapshots, one can see that domain growth slows down considerably with increasing disorder.

Next, we present results for the correlation function, which is defined in Eq. (8). As the system is isotropic, we spherically average the vector function $C(\vec{r},t)$ to obtain the scalar function $C(r,t)$. In Fig. 3(a), we plot $C(r,t)$ vs r/L at different times for $W = 0.125$. The length scale L is defined as the distance over which $C(r,t)$ decays to $0.2\times$ maximum value. The neat data collapse confirms that dynamical scaling applies

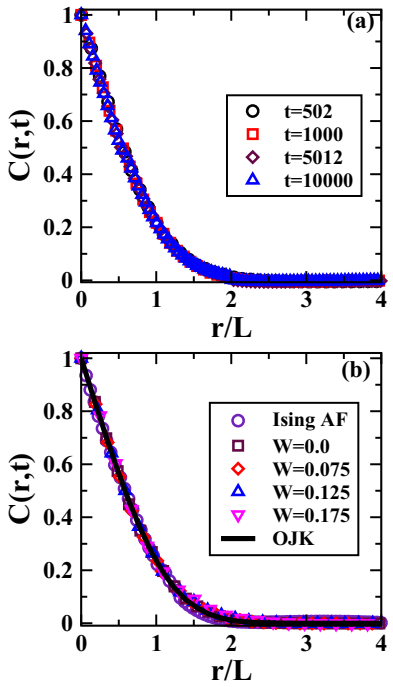

FIG. 3. (a) Scaled correlation functions $[C(r,t)$ vs $r/L]$ for disorder $W = 0.125$ and four different times. The length scale L is defined as the distance over which $C(r,t)$ decays to $0.2 \times$ maximum value. (b) Scaled correlation functions at $t = 10^3$ MCS for $W = 0.0,\ 0.075,\ 0.125$, and 0.175. For comparison, we also present data for the Ising AF with Kawasaki kinetics at $t = 502$ MCS. The solid line denotes the OJK function in Eq. (10).

for this system. In Fig. 3(b), we compare the scaling functions at $t = 10^3$ MCS for different disorder amplitudes: $W = 0.0, 0.75, 0.125, 0.175$. We also superpose data for the NN Ising AF and the OJK function in Eq. (10) (solid line). We see that the scaling functions are numerically indistinguishable. This demonstrates the following.

(a) The evolution morphologies for the CG with different disorder amplitudes are the same, and only differ in the length scale. This property has been termed as "superuniversality" (SU) [7].

(b) The scaling function for the CG with Kawasaki kinetics is the same as that of the NN Ising model with Glauber kinetics, showing that they belong to the same nonequilibrium universality class.

Before proceeding, we should stress that Corberi *et al.* [9,10] have found that the SU property does not apply to the two-time autocorrelation functions in the NN RFIM and RBIM. A similar breakdown of SU is expected for the long-ranged CG model studied in this paper.

Let us next investigate the time dependence of domain growth. In Fig. 4, we plot $L(t)$ vs t for the CG with $W = 0.0, 0.075, 0.125, 0.175$. For the pure case ($W = 0$), our data obeys the LCA law ($L \sim t^{1/2}$), which was proposed for the NN Ising model. For the disordered cases, the growth is slower and clearly does not obey a power law, which would show as a linear trend on the log-log plot of Fig. 4. In Fig. 5(a), we plot $z_{\rm eff}$ defined in Eq. (26) vs t on a log-linear scale. For the pure case, the data levels at $z_{\rm eff} = 2$, as expected. This

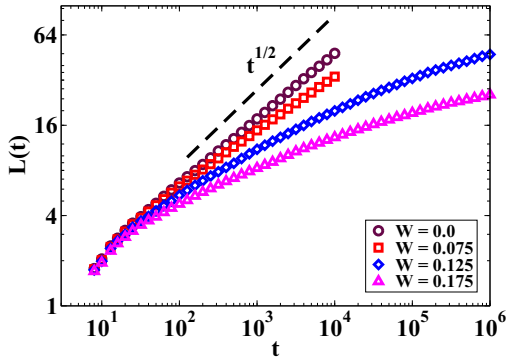

FIG. 4. Log-log plot of $L(t)$ vs t for the $d = 2$ CG at different W. The dashed line denotes the LCA growth law, $L(t) \sim t^{1/2}$.

corresponds to $\bar{z} = 2$ and $\lambda \to \infty$. For higher values of W, there is a regime where $z_{\rm eff} = \bar{z}$ (constant), followed by an upward trend in $z_{\rm eff}$ vs t. The time window ($t < t_0, L < \lambda$) over which $z_{\rm eff}$ is constant becomes smaller as W increases. In Table I, we present values of $\bar{z}$ for different values of W/T. These are plotted in Fig. 5(b). We see that $\bar{z} = 2 + cW/T$, where c is a constant. This is in agreement with the results of Paul *et al.* [8] for the NN RBIM. In Fig. 5(c), we plot $z_{\rm eff} - \bar{z}$ vs L/λ for different W. The parameters λ are chosen so as to enable a data collapse—their values are provided in Table I. The collapsed data sets are well described by a power-law function:

$$z_{\rm eff} - \bar{z} \simeq b\left(\frac{L}{\lambda}\right)^{\psi}, \tag{29}$$

which is denoted by a solid line. The best-fit parameters are $b \simeq 0.53$ and $\psi \simeq 2.10$. As we have discussed in Sec. III, this

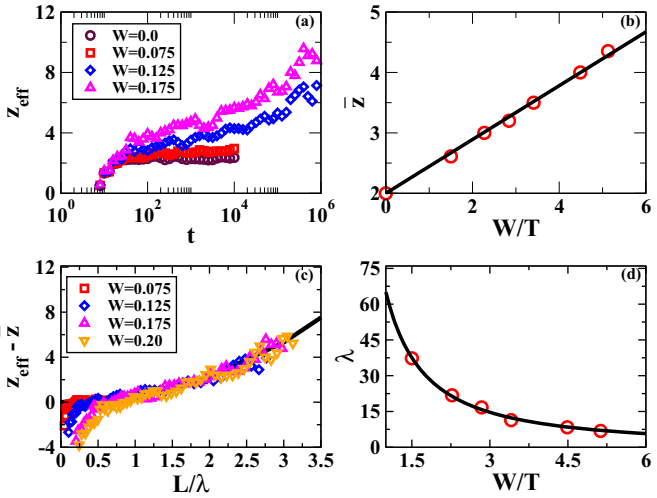

FIG. 5. (a) Effective exponent $z_{\rm eff}$ vs t in the $d = 2$ CG. (b) Plot of $\bar{z}$ vs W/T. The solid line denotes the best linear fit: $\bar{z} = 2 + 0.45W/T$. (c) Plot of $(z_{\rm eff} - \bar{z})$ vs L/λ. The λ values are chosen to obtain a data collapse and their values are given in Table I. The solid line is the best fit: $z_{\rm eff} - \bar{z} = 0.53(L/\lambda)^{2.1}$. (d) Plot of λ vs W/T. The solid line is the best fit $\lambda \sim (W/T)^{-1.36}$.

TABLE I. Values of parameters $\bar{z}$ and λ for the CG at different W/T.

W	W/T	$\bar{z}$	λ
0.0	0.0	2	∞
0.075	1.50	2.61	37.28
0.10	2.27	3.00	21.77
0.125	2.84	3.20	16.68
0.15	3.40	3.50	11.36
0.175	4.48	4.00	8.36
0.20	5.12	4.35	6.82

corresponds to the asymptotic growth law

$$L(t) \sim \left[\ln\left(\frac{t}{t_0}\right)\right]^{1/\psi}. \tag{30}$$

For the NN RFIM in $d = 2$, Corberi *et al.* [10] have estimated the corresponding logarithmic growth exponent as $\psi \simeq 1.5$ and the relevant analytic prediction is $\psi = 1$ [37,38]. Our value for ψ is of the same order as that predicted analytically and numerically for the NN RFIM. It should be kept in mind that the system studied here has long-ranged Coulombic interactions. This may result in minor differences from the NN RFIM. Alternatively, this discrepancy could arise from the numerical difficulty in precisely calculating logarithmic exponents rather than any fundamental differences in these two models. Finally, in Fig. 5(d), we plot λ vs W/T. The data obeys a power-law behavior with the best-fit $\lambda \sim (W/T)^{-1.36}$.

V. SUMMARY AND DISCUSSION

We have studied the coarsening kinetics of a $d = 2$ Coulomb glass (CG) at half-filling using Monte Carlo (MC) simulations. The summary of our results is as follows.

(a) The domain morphology in the CG, which is an antiferromagnet (AF) with long-range Coulombic interactions, is analogous to the morphology in the NN Ising AF with Kawasaki kinetics. Further, the latter model is equivalent to the NN Ising ferromagnet with Glauber kinetics.

(b) The domain growth law shows a crossover from a regime of "power-law growth with disorder-dependent exponent" ($L \sim t^{1/\bar{z}}$) to a regime of "universal logarithmic growth" [$L \sim (\ln t)^{1/\psi}$]. A similar behavior has been seen for the NN RFIM [10], though there is a slight disagreement in the logarithmic exponents. A microscopic theory to explain the crossover still does not exist. Such a theory would provide a basis for the energy-barrier scaling in Eq. (13) and a precise estimate of the numerical prefactors and the scaling exponent ψ. In turn, this would yield the complete scaling forms (with prefactors) of the crossover functions: $F(x)$ in Eq. (21) and $G(y)$ in Eq. (23).

As mentioned earlier, at zero disorder the critical exponents of the CG are found to be the same as those of the NN Ising model [23]. We believe that this universality extends to the nonequilibrium properties. This may be attributed to the cancellation of long-ranged interactions due to the checkerboard ground state of the AF, rendering the CG Hamiltonian equivalent to the NN Hamiltonian. (This does not apply to the ferromagnetic model where Coulombic interactions change both the static and dynamic properties).

For nonzero disorder, two of us [26] have found that the $d = 2$ CG has a phase transition at nonzero disorder ($W_c > 0$) at $T = 0$. This should be contrasted with the NN RFIM in $d = 2$, where $W_c = 0$ at $T = 0$. However, as far as domain growth in $d = 2$ is concerned, the properties of the CG and the NN RFIM are analogous.

We next plan to study domain growth in the CG with asymmetric composition, i.e., with a surplus of holes or electrons. In this case, the order parameter (no longer the staggered magnetization) remains a nonconserved quantity during the evolution. However, the conserved composition plays a nontrivial role in the ordering dynamics of asymmetric systems [33]. Another important factor in the asymmetric CG is that the long-ranged term does not drop out due to cancellation of alternating terms. Therefore, we expect several different features in the ordering kinetics of the asymmetric CG. One can also extend this work to intermediate and high disorders, where the system is expected to show glassy behavior. In that context, one would have to look for alternative order parameters and quantities to characterize the "domain" growth. These would also be relevant to other glassy systems.

ACKNOWLEDGMENT

S.P. is grateful to the Department of Science and Technology, India, for funding via a J.C. Bose Fellowship

[1] *Kinetics of Phase Transitions*, edited by S. Puri and V. K. Wadhawan (CRC Press, Boca Raton, FL, 2009).
[2] A. J. Bray, Adv. Phys. **43**, 357 (1994).
[3] S. Dattagupta and S. Puri, *Dissipative Phenomena in Condensed Matter: Some Applications* (Springer-Verlag, Berlin, 2004).
[4] Z. W. Lai, G. F. Mazenko, and O. T. Valls, Phys. Rev. B **37**, 9481 (1988).
[5] D. A. Huse and C. L. Henley, Phys. Rev. Lett. **54**, 2708 (1985).
[6] S. Puri, Phase Transit. **77**, 469 (2004).
[7] S. Puri, D. Chowdhury, and N. Parekh, J. Phys. A: Math. Gen. **24**, L1087 (1991); S. Puri and N. Parekh, *ibid.* **25**, 4127 (1992).
[8] R. Paul, S. Puri, and H. Rieger, Europhys. Lett. **68**, 881 (2004); Phys. Rev. E **71**, 061109 (2005).
[9] E. Lippiello, A. Mukherjee, S. Puri, and M. Zannetti, Europhys. Lett. **90**, 46006 (2010); F. Corberi, E. Lippiello, A. Mukherjee, S. Puri, and M. Zannetti, J. Stat. Mech.: Theory Exp. (2011), P03016.
[10] F. Corberi, E. Lippiello, A. Mukherjee, S. Puri, and M. Zannetti, Phys. Rev. E **85**, 021141 (2012).
[11] A. L. Efros and B. I. Shklovskii, J. Phys. C: Solid State Phys. **8**, L49 (1975).
[12] B. I. Shklovskii and A. L. Efros, *Electronic Properties of Doped Semiconductors* (Springer, Heidelberg, 1984).

[13] M. Pollak, M. Ortuño, and A. Frydman, *The Electron Glass* (Cambridge University Press, Cambridge, UK, 2013).
[14] M. Ben-Chorin, Z. Ovadyahu, and M. Pollak, Phys. Rev. B **48**, 15025 (1993).
[15] G. Martinez-Arizala, C. Christiansen, D. E. Grupp, N. Markovic, A. M. Mack, and A. M. Goldman, Phys. Rev. B **57**, R670 (1998).
[16] T. Grenet, Eur. Phys. J. B **32**, 275 (2003).
[17] A. Vaknin, Z. Ovadyahu, and M. Pollak, Phys. Rev. Lett. **84**, 3402 (2000).
[18] M. T. Shimer, U. C. Tauber, and M. Pleimling, Phys. Rev. E **90**, 032111 (2014).
[19] T. Grenet, Phys. Status Solidi C **1**, 9 (2004).
[20] Z. Ovadyahu, Phys. Rev. B **73**, 214204 (2006).
[21] A. Vaknin, Z. Ovadyahu, and M. Pollak, Phys. Rev. B **65**, 134208 (2002).
[22] E. Lebanon and M. Muller, Phys. Rev. B **72**, 174202 (2005).
[23] A. Mobius and U. K. Rossler, Phys. Rev. B **79**, 174206 (2009).
[24] M. Goethe and M. Palassini, Phys. Rev. Lett. **103**, 045702 (2009).
[25] P. Bhandari and V. Malik, arXiv:1708.01169.
[26] P. Bhandari, V. Malik, and S. R. Ahmad, Phys. Rev. B **95**, 184203 (2017).
[27] J. Z. Imbrie, Phys. Rev. Lett. **53**, 1747 (1984); Commun. Math. Phys. **98**, 145 (1985).
[28] J. Bricmont and A. Kupiainen, Phys. Rev. Lett. **59**, 1829 (1987).
[29] D. Frenkel and B. Smit, *Understanding Molecular Simulations: From Algorithms to Applications* (Academic Press, San Diego, 1996).
[30] K. Binder and D. W. Heermann, *Monte Carlo Simulation in Statistical Physics: An Introduction*, 4th ed. (Springer-Verlag, Berlin, 2002).
[31] M. E. J. Newman and G. T. Barkema, *Monte Carlo Methods in Statistical Physics* (Oxford University Press, Oxford, 1999).
[32] J. F. Marko and G. T. Barkema, Phys. Rev. E **52**, 2522 (1995).
[33] P. Das, T. Saha-Dasgupta, and S. Puri, Eur. Phys. J. E **40**, 94 (2017).
[34] T. Ohta, D. Jasnow, and K. Kawasaki, Phys. Rev. Lett. **49**, 1223 (1982).
[35] C. L. Henley, Phys. Rev. Lett. **54**, 2030 (1985).
[36] J. D. Shore, M. Holzer, and J. P. Sethna, Phys. Rev. B **46**, 11376 (1992).
[37] J. Villain, Phys. Rev. Lett. **52**, 1543 (1984).
[38] G. Grinstein and J. F. Fernandez, Phys. Rev. B **29**, 6389 (1984).